

A study on fracture characteristics of micron diamond powders under static high pressure conditions

Ion C. Benea, Ph.D., Benjamin R. Rosczyk

Engis Corporation, Wheeling, IL 60090, USA

1. Abstract

The manufacturing process of polycrystalline diamond compacts (PDC) consists primarily in sintering of micron size diamond particles into a coherent and homogeneous polycrystalline diamond (PCD) layer on top a tungsten carbide substrate, under high pressure and high temperature conditions (i.e. $P > 5.5$ GPa; $T > 1,400$ °C).

During ramp-up to sintering pressure at room temperature, many diamond particles are crushed, due to compression and shear stresses. Thus, subsequent to pressure ramp-up, particle size distribution of the precursor micron diamond powder withstands a significant change.

Consequently, besides the HPHT sintering process, fracture characteristics (fracture strength and mode) of precursor micron diamond powder used for high pressure-high temperature (HPHT) sintering of PCD layer, may have a critical contribution to impact strength and abrasion resistance of polycrystalline diamond compacts (i.e. PDC cutters for oil and gas drilling, PDC tool blanks and dies, etc.).

Current technique used to assess the fracture strength and mode of micron diamond powders is based on subjecting the micron diamond powder sample to mechanical forces similar to those encountered in the lapping process [1, 2]. This technique is based on crushing a, virtually, single layer of diamond particles between two sintered polycrystalline diamond surfaces, which rotate in opposite direction, under low compressive force. Thus, larger particles are crushed, mainly due to shear stresses, while smaller particles are not crushed.

The objective of this study is to develop a high pressure apparatus designed to study the fracture characteristics of micron diamond powders under high pressure, and the associated technique to measure the crushing strength of micron diamond powder under static high pressure conditions, corresponding to those used for HPHT sintering of PDC. The crushing strength was investigated by subjecting different micron size diamond powder samples to static high pressure conditions. Prior to high pressure treatment, micron size diamond powder samples were characterized with respect to particle size, particle shape and concentration of crystalline defects. After high pressure treatment, micron diamond powder samples were characterized with respect to particle size distribution to determine the crushing characteristics – high pressure crushing strength index (HP-CSI), and size distribution of crushed diamond particles.

Understanding the fracture strength and mode of micron diamond powder under static high pressure conditions, is regarded as a prerequisite for the development of precursor micron diamond powders whose properties are designed and controlled to ensure predictable and consistent performance under the high pressure conditions, particular to different PDC sintering processes.

2. Experimental

2.1 High pressure apparatus design

For the purpose of this study, an opposed anvils high pressure apparatus was design and built. The opposed anvils high pressure apparatus, known as Bridgman anvils, is considered as ideal for high pressure generation, due to its simplicity and unlimited stroke, which allows unlimited compression of the pressure media. In its original design, the main disadvantage of Bridgman anvils apparatus, is represented by the small volume of the sample subjected to compression. Opposed anvils apparatus can generate high pressures that exceed the compressive strength of the tungsten carbide (WC), from which anvils are made. This is possible through combination of the effect of “massive support” with the effect of lateral support. According to the principle of massive support, if the high pressure is generated on a small area of a much larger body, then, compressive stress of two to three times the compressive yield stress of the material can be supported.

The relationship between anvil’s geometry and massive support, is defined by the constant of massive support (M):

$$M = \Omega / 2\pi$$

where, Ω is the solid angle of the conical anvil.

The constant of massive support reaches its maximum value $M = 1$, for $\Omega = 2\pi$ or 0° bevel angle of the anvil’s face.

The geometry of the WC-6%Co anvils was chosen to maximize the effect of massive support and, at the same time, to prevent indentation of the WC anvil into adjacent steel surfaces under maximum force applied on anvils.

In this design, the anvil’s face bevel angle is chosen 12° , which corresponds to a solid angle, $\Omega = 1.14\pi$, and to a massive support constant, $M = 0.57$.

The minimum diameter of the CW anvil is calculated using the formula:

$$R_a = (F_{\max} / \pi \times \sigma_{p02})^{1/2}$$

A 40-ton automatic hydraulic press capable of delivering a maximum force of 40 tf ($3,92 \cdot 10^5$ N), was employed in conjunction with this high pressure apparatus.

The yield strength, $\sigma_{p0,2} = 1,63 \cdot 10^3$ MPa ($1,63 \cdot 10^3$ N/mm²), was chosen for the adjacent steel surfaces in contact with WC anvils. Hence, the calculated minimum radius of the WC anvil is: $R_a = 7.9$ mm. Therefore, the minimum diameter of the WC anvil should be more than 15.8 mm.

Given the main purpose of this high pressure apparatus, that of crushing of micron size diamond powders, a PDC cutter was inserted in the central face area of each WC anvil, to prevent indentation of diamond particles into anvil’s face. Thus, micron diamond particles are crushed between two sintered polycrystalline diamond surfaces, on which the force needed for high pressure generation, is applied.

The added benefit of using composite PDC-WC-6%Co anvils, consists in the extension of the high pressure range of this apparatus.

Main mechanical properties of sintered WC-6%Co and PCD (polycrystalline diamond layer of the PDC cutter), are presented in table 1.

Table 1. Mechanical properties of WC-6%Co and PCD

	WC-6% Co	PCD
Hardness	1,620 HV30	49.8 GPa Knoop
Compressive strength (GPa)	~ 5.5	6.9 – 7.7
Modulus of rigidity (GPa)	-	426
Young modulus (GPa)	630	890
Poisson coefficient	0.22	0.086

The geometry and dimensions of the composite PDC-WC anvil are shown in Fig. 1, while in Fig. 2a and 2b pictures of composite PDC-WC anvils, PDC cutter are presented. Fig. 2c, exhibits a SEM micrograph of the PDC layer.

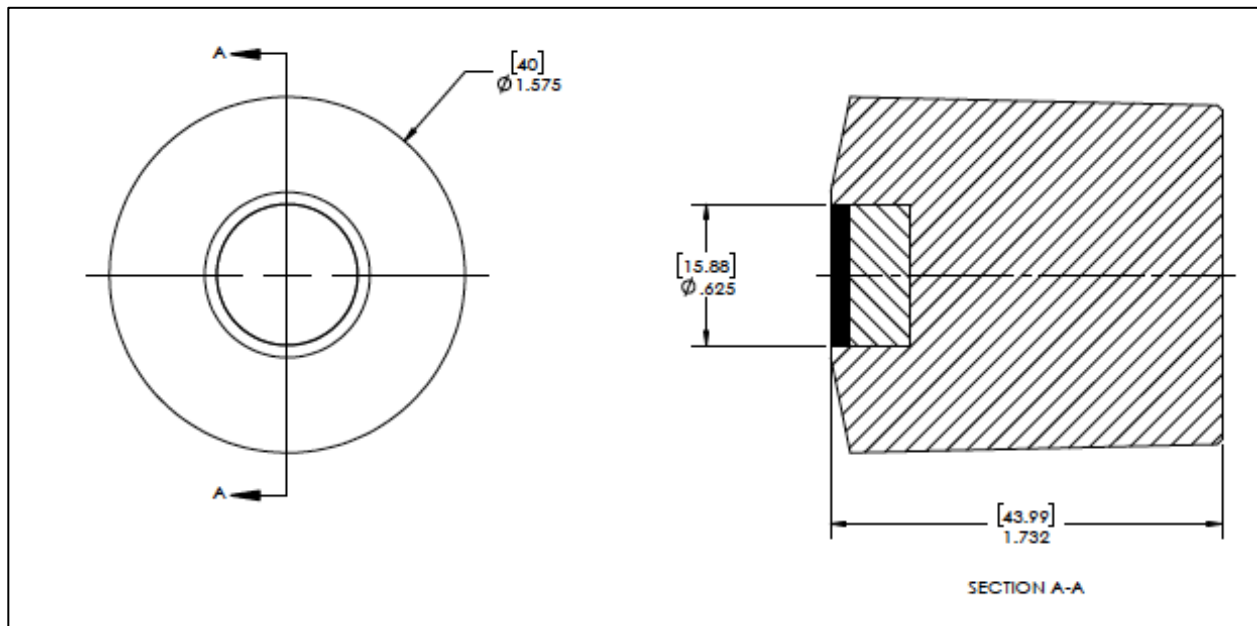


Fig. 1 – Composite PDC-6%WC anvil



Fig 2a



Fig 2b

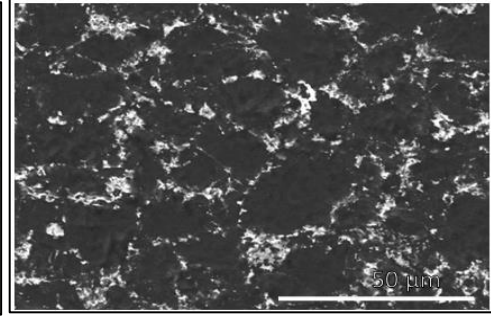


Fig 2c

The lateral support of the anvil can be delivered by applying a lateral force on the cylindrical surface of the anvil, as well as, on the tapered surface of the anvil. Only the lateral support on the cylindrical surface of the anvil was used for this design.

Finite Element (FE) analysis was used to analyze stresses within the WC anvil body and to determine the lateral support pressure on the cylindrical surface of the WC anvil.

The 3D model used for FE analysis is presented in Fig. 3a. The equivalent stress distribution within the WC anvil, generated when 40 tf is applied on the face of the WC anvil is shown in Fig. 3b.

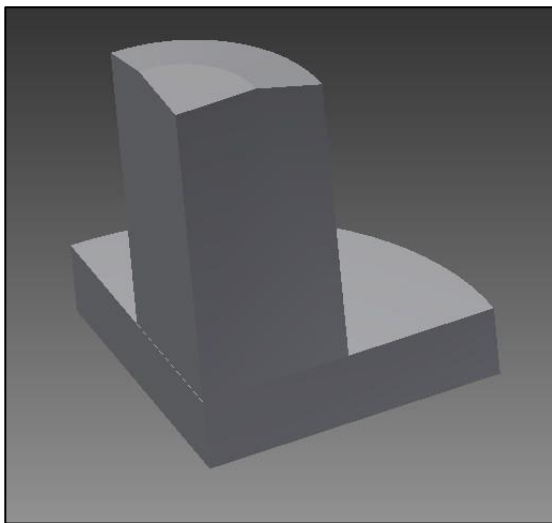


Fig. 3a – 3D model of WC anvil

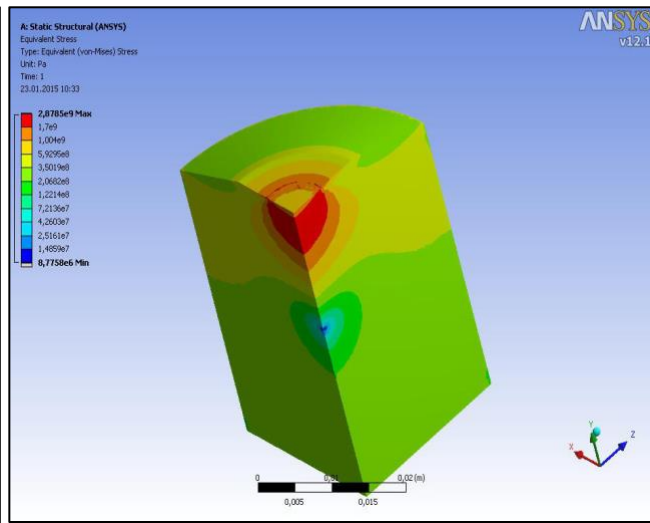


Fig. 3b – equivalent stress distribution

From FE analysis, the lateral support pressure to pre-stress the WC anvil was chosen to be approx. $5 \cdot 10^8 \text{ N/m}^2$ (0.5 GPa), to prevent development of compressive stresses above material's limit, as well as, development of tensile and compressive stresses to a level that would damage the WC anvil under maximum applied load. The lateral support applied on the cylindrical surface of the anvil, was provided by a set of two high strength steel (HSS) binding rings which were press fitted onto the CW anvil – Fig. 4a and 4b.

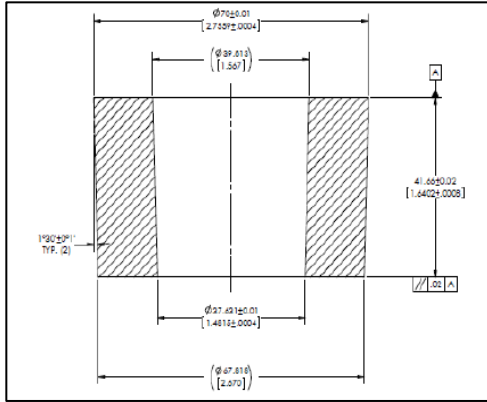


Fig. 4a – HS steel ring #1

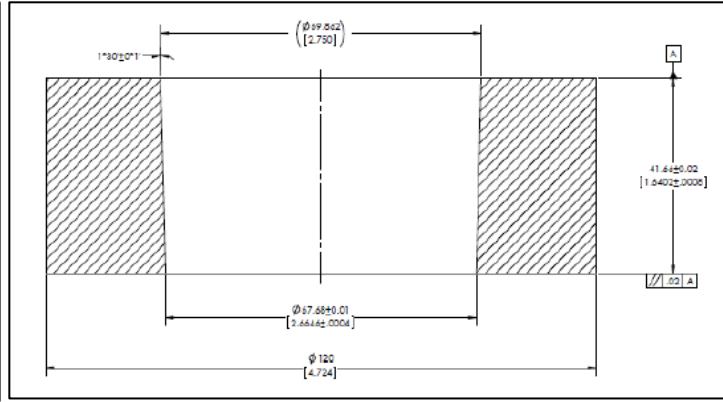


Fig. 4b – HS steel ring #2

A guiding-containing device was also designed and built to assure alignment and concentricity of the two opposed anvils, as well as, to prevent ejection of any fragments of materials in case of a blowout during pressing cycle. The inner wall of the guiding device was lined with Teflon foil to electrically insulate the two anvil assemblies.

2.2 Sample cell assembly

The high pressure diamond crushing experiments were conducted using a sample cell assembly which consists of a compressible gasket made of soft steel (8 mm internal diameter, 11 mm outside diameter and 2.5 mm thickness), in which the micron diamond powder sample is loaded, Fig. 5.

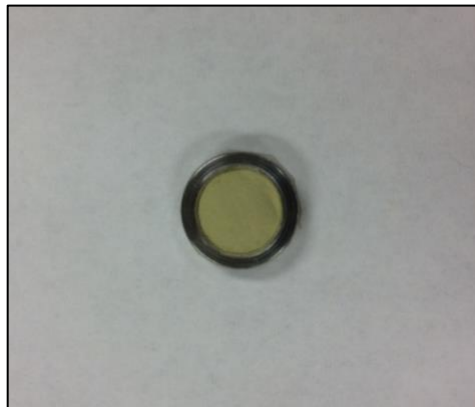


Fig. 5 – Sample cell for HP crushing strength measurement of micron diamond powder

The assembled high pressure crushing strength (HP-CS) apparatus (comprised of WC anvils pre-stressed with high strength steel rings and guiding-containing device), and the sample cell for diamond crushing under high pressure, is pictured in Fig. 6.



Fig. 6 – HP-CS apparatus and sample cell

Attempts to measure the pressure generated on the sample cell assembly used in this study (diamond powder charged inside the steel gasket), failed due to shear of the pressure sensor (Bi strip) and electrical contacts (Cu strips). On the other hand, pressure measurement on a sample cell assembly in which diamond powder is replaced by a pressure transmitting media (i.e. NaCl, hBN, MgO, pyrophyllite, etc.), would not be relevant for this study, since the pressure generated would be much lower. The reason for that, resides in the large difference between compressive strength of diamond and compressive strength of pressure media (i.e. NaCl, hBN, MgO, pyrophyllite, etc.).

Given the relative nature of the crushing strength test, pressure calibration is of a much lesser importance than the reliability and repeatability of the test.

Calculated average pressure as a function of applied force, on 8 mm circular area and 11 mm circular area, is illustrated in Fig. 7.

Pressure generated on the diamond powder samples was instead estimated indirectly by comparing the results of our HP crushing experiments, expressed as high pressure crushing strength index (HP-CSI), with the HP-CSI results obtained by crushing same diamond powder samples using an industrial cubic press for PDC sintering, which was previously calibrated with respect to pressure generated within sample cell (synthetic pressure media cube), as a function of press force.

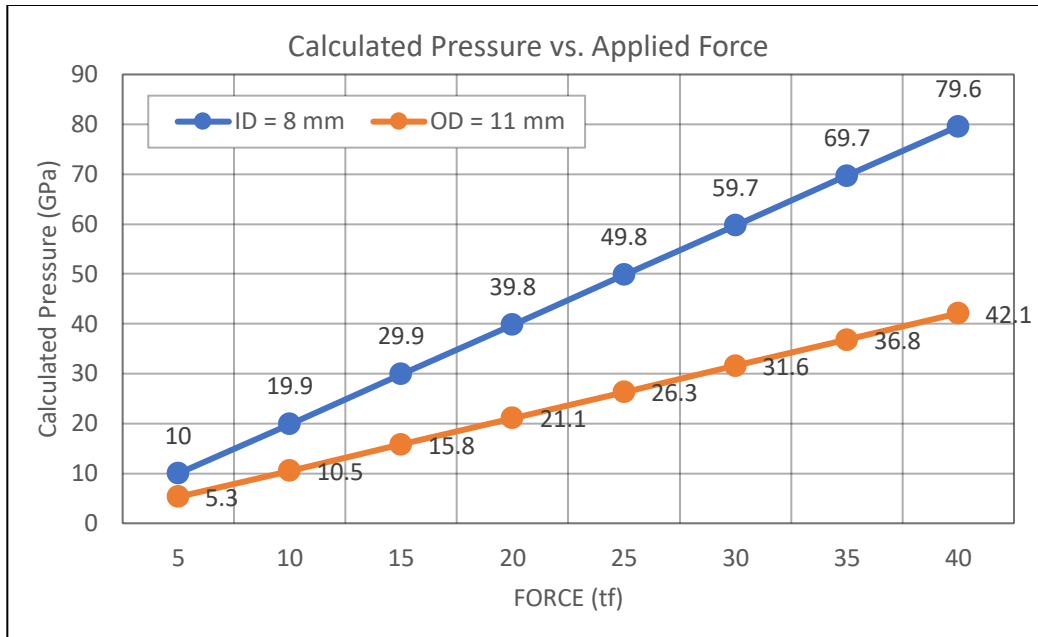


Fig. 7 – Average calculated pressure vs. applied force

It is known that maximum pressure is generated on the inner part of the gasket, while the pressure at the edge of the gasket is equal to atmospheric pressure. Thus, plastic flow occurs at the outer part of the compressible gasket. The pressure gradient which is produced in the plastic flow region seals the pressure of the inner part.

Given the shear modulus of rigidity of diamond (i.e. $G = 476 \text{ GPa}$), the load is first distributed on diamond powder sample. As a result, packing density of diamond powder sample increases due to particle crushing; the volume of the diamond powder sample decreases. Consequently, extrusion of the steel gasket is directly related to the extent the diamond particles crush. Once crushing of diamond particles is completed, there is no more extrusion of the steel gasket.

Images of the sample cell before and after high pressure crushing of $30 \mu\text{m}$ diamond powder is shown in Fig. 8. Change in color of diamond sample is likely due to fine particles resulted from crushing of larger particles.

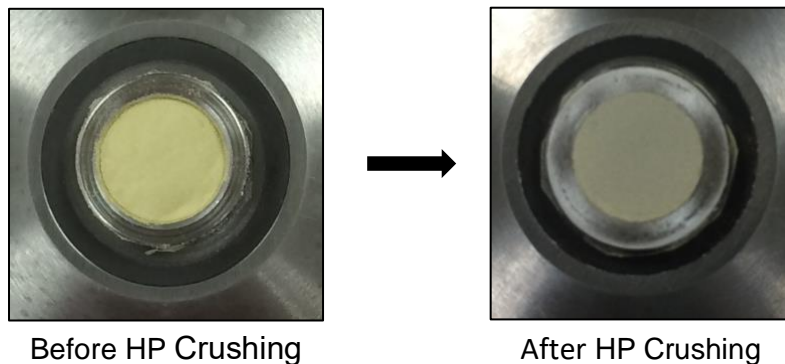


Fig. 8 – Sample cell before and after HP crushing of $30 \mu\text{m}$ diamond powder

The dimensions of the steel gasket with and without diamond powder (average of three measurements), following compression at 15 tf. are presented in table 2.

Table 2.

F = 15 tf; t = 60 sec.	ID (mm)	OD (mm)	t (mm)
Steel gasket with diamond powder	8.03	12.34	1.78
Steel gasket without diamond powder	6.59	13.35	1.09

3. Experimental Procedure

3.1 HP-CSI test procedure

Diamond powder samples were crushed by placing a known mass of diamond powder inside the steel gasket. The sample cell assembly (diamond plus steel gasket) was inserted between the two PDC-WC composite anvil assemblies positioned within the guiding-containing device. The whole assembly was then placed in an automatic 40 ton hydraulic press and the desired load was applied for the test duration, Fig. 9.

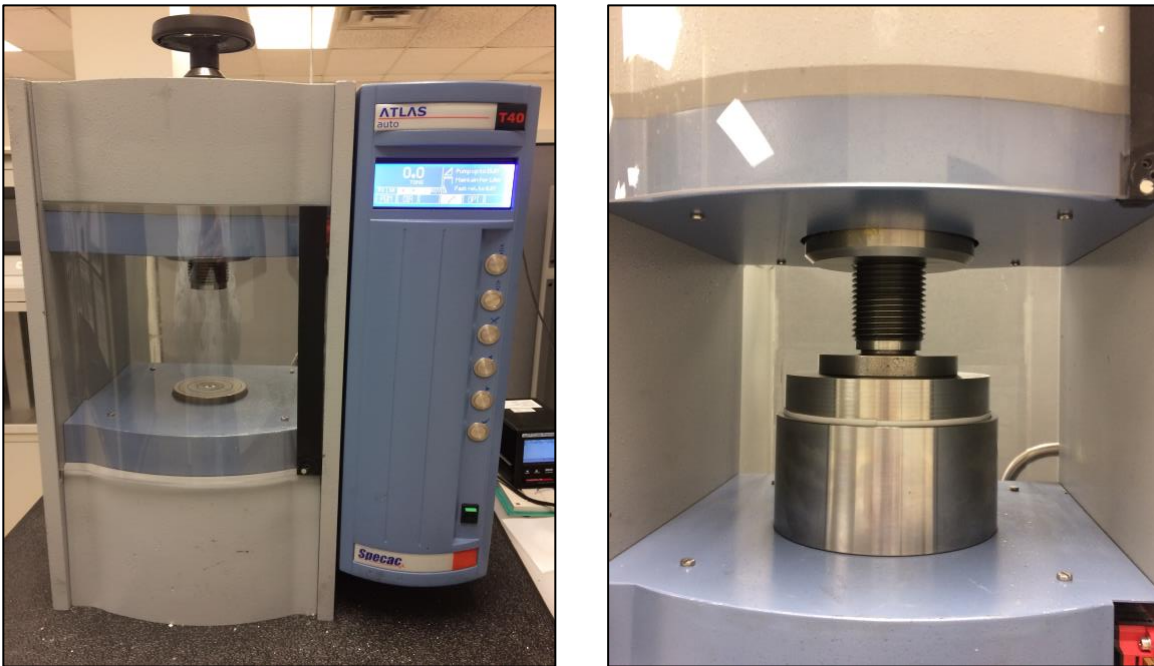


Fig. 9 – Automatic 40-ton hydraulic press and high pressure apparatus

After high pressure treatment, the crushed diamond powder was recovered for particle size measurement.

Particle size distribution (number distribution) of the starting (uncrushed) and crushed diamond powder was measured using a Beckman Coulter Multisizer III. The High Pressure Crushing Strength Index (HP-CSI) was calculated using the formula:

$$\text{HP-CSI} = \text{ROS}/\text{IOS} \times 100$$

where, IOS is the total number of particles between the median (D50) and the D95 of the particle size distribution of the starting (uncrushed) powder, and ROS is the total number of uncrushed particles, within the same size range, resulted after high pressure treatment, Fig. 10.

All HP-CSI values were determined from the average of three (3) trials with the standard deviation between trials used as the measurement error.

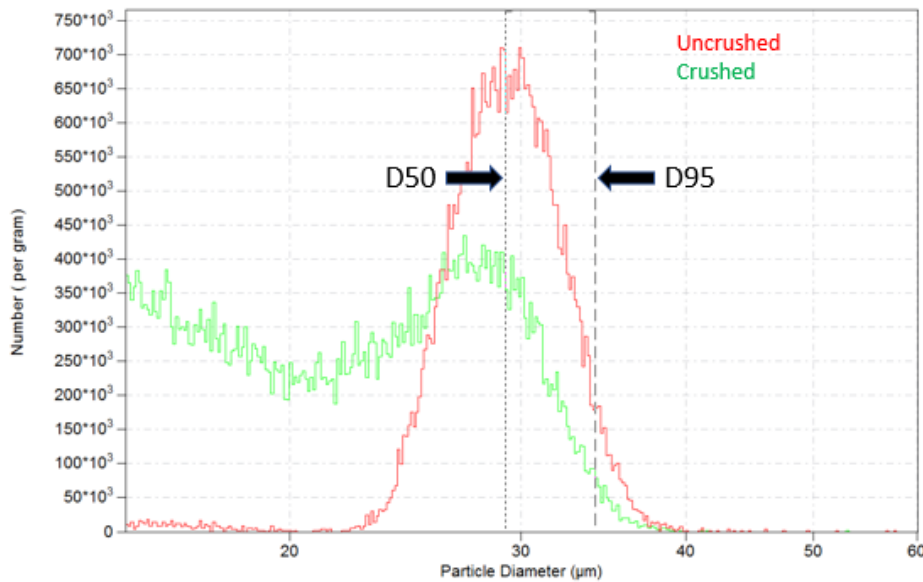


Fig. 10 – Calculation of HP-CSI

To assess the repeatability of the high pressure crushing strength apparatus, a 0.220 ± 0.001 g of 30 μm monocrystalline metal bond diamond powder was crushed five times at 15 tf for 60 seconds. The crushed powder was collected for particle size measurement.

Table 3 – Repeat HP-CSI measurements on 30 μm diamond powder sample

Trial	HP-CSI (%)	Std. Dev. (%)
1	45.1%	1.0%
2	42.6%	1.4%
3	43.2%	1.1%
4	44.9%	1.5%
5	44.2%	1.1%

The average HP-CSI over all five measurements was $44.0\% \pm 1.1\%$. The standard deviation between measurements was considered acceptable because it was similar in magnitude to the standard deviation between individual measurement within each test (1-1.5%).

3.2 Comparison HP-CS apparatus vs. industrial cubic press for PDC sintering

Monocrystalline metal bond diamond powder samples, ranging in size from 12 μm to 30 μm , were crushed both in an industrial cubic press for PDC sintering at 5.0 and 6.0 GPa for 60 seconds and the HP-CSI apparatus at 15 tf for 60 seconds. All crushed samples were collected and the HP-CSI was calculated for each sample, Fig. 11.

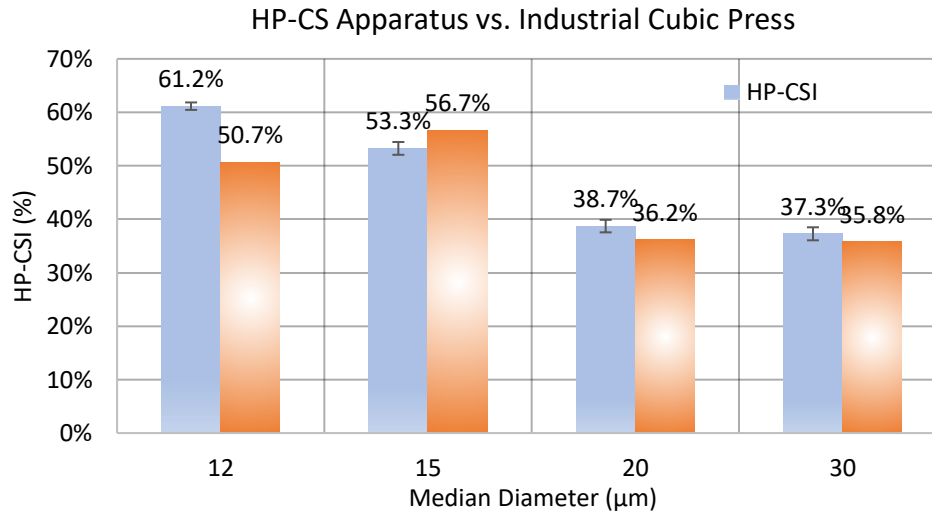


Fig. 11 – Comparison of HP-CS apparatus with industrial cubic press for PDC sintering

Same diamond powder samples, experienced a similar degree of crushing when crushed at 5.0 and 6.0 GPa in an industrial cubic press for PDC sintering, and when crushed at 15 tf in the HP-CS apparatus. Therefore, diamond crushed at 15 tf in the HP-CS apparatus may display similar crushing characteristics (crushing strength and mode), that would be observed in an industrial cubic press during PDC sintering.

3.3 HP-CSI test parameters

To explore the capabilities of the technique developed to measure the HP-CSI, micron diamond crushing experiments were conducted at different loads, different dwell times, and on different micron diamond sizes.

a) Applied Load

A 0.220 ± 0.001 g of 30 μm monocrystalline metal bond diamond powder was crushed under loads ranging from 10 tf to 30 tf and constant dwell time of 60 seconds.

HP-CSI of 30 μm monocrystalline metal bond diamond powder as a function of applied load is presented in Fig. 12.

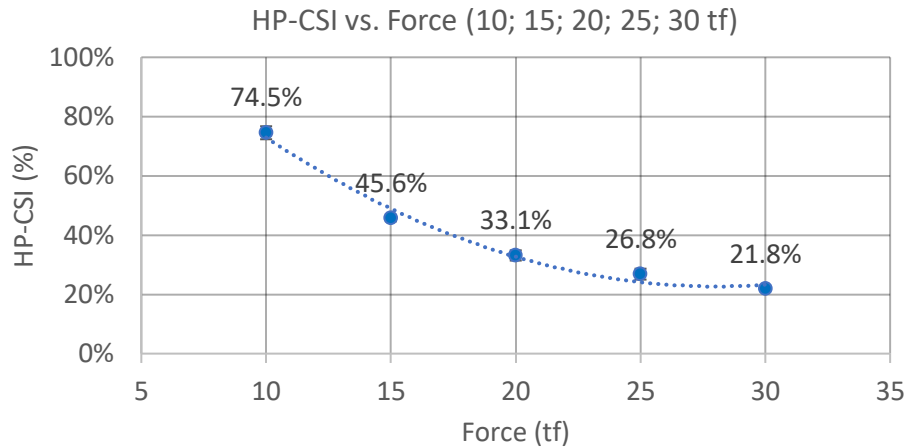


Fig. 12 – HP-CSI with applied load at constant dwell time

There is a non-linear relationship between HP-CSI and applied load; HP-CSI decreases when load increases.

b) Dwell time

The same 30 μm monocrystalline metal bond diamond powder was crushed at a constant load of 15 tf and different dwell times. It was found that, under constant load of 15 tf, HP-CSI decreases when dwell time increases from 60 seconds to 600 seconds, indicating that diamond fracture is a continuous process when applied load is kept constant, Fig. 13.

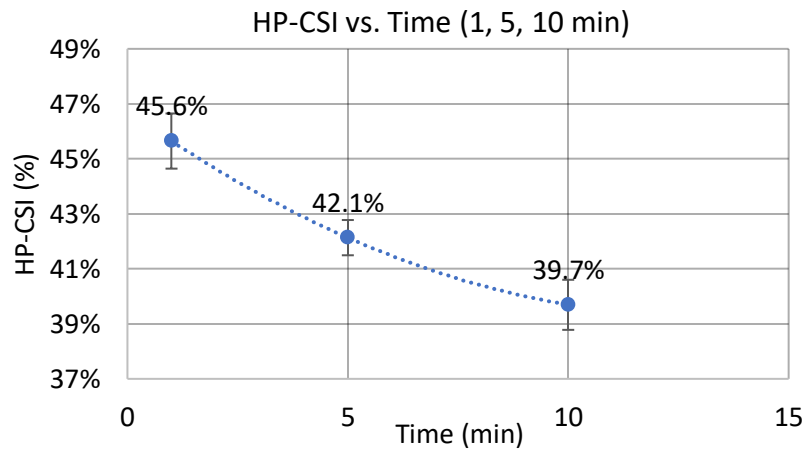


Fig. 13 – HP-CSI with time at constant load

c) Diamond size

Monocrystalline metal bond diamond powder samples ranging in size from 6 μm to 30 μm were crushed under identical conditions of 15 tf and 60 s.

Slightly less mass was used for the HP-CSI testing of the 6 μm and 12 μm samples due to the difference in bulk density (packing density) of smaller particle sizes. As expected, HP-CSI increases as particle size decreases, Fig. 14.

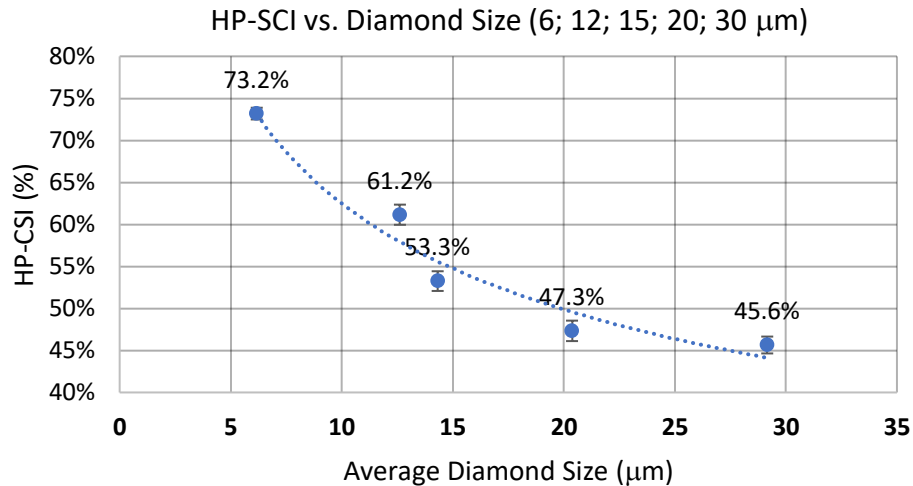


Fig. 14 – HP-CSI with diamond size at constant load and dwell time

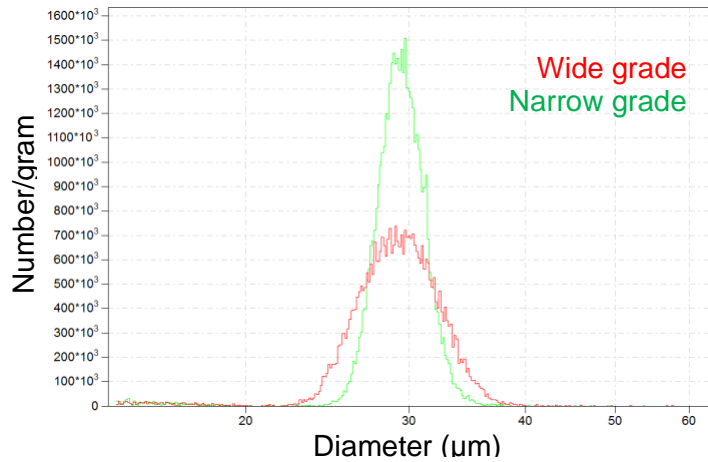
3.3 HP-CSI experiments

To study the effect of particle size distribution, particle shape and concentration of residual crystal growth defects (RCGD) on crushing strength and mode of diamond particles under static HP, the following crushing experiments were conducted on 30 μm monocrystalline diamond powder, at 15 tf and 60 seconds:

- Particle Size Distribution (PSD width): narrow vs. wide PSD
- Particle shape (aspect ratio – AR): high vs. normal AR
- Concentration of residual crystal growth defects (DR-FTIR baseline transmittance – BT): high vs. low BT

a) Effect of PSD width on HP-CSI

To study the effect of the particle size distribution (PSD width) on the crushing characteristics of diamond powder at high pressure, a monocrystalline diamond powder feed lot was sized into a narrow and wide particle size distribution while the median (D50) was maintained at approx. 30 μm , Fig. 15. Analysis of the particle shape confirmed that the average aspect ratio remained nearly identical.



Sample	Diameter on % (μm)		
	5%	50%	95%
Narrow Grade	26.63	29.35	32.32
Wide Grade	24.82	29.19	34.09

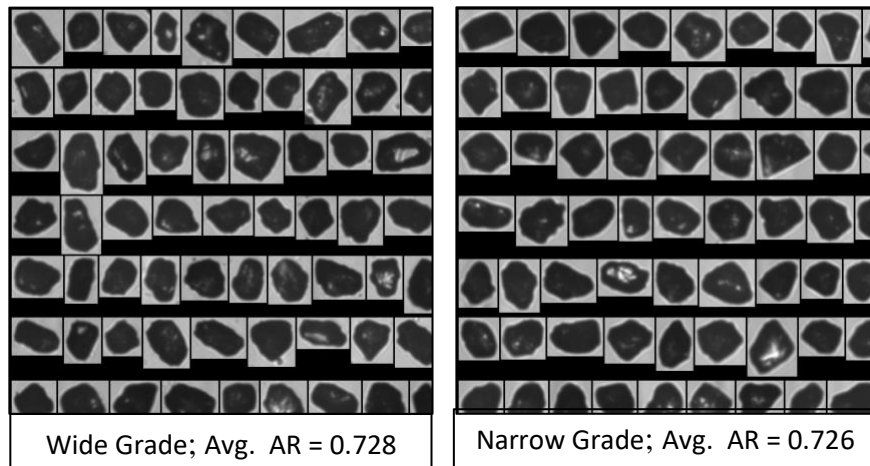


Fig. 15 – PSD and particle shape of 30 μm diamond samples – wide vs. narrow PSD

The HP-CSI of the narrow distribution 30 μm powder was found to be significantly lower than the HP-CSI of the wide distribution 30 μm powder, Fig. 16 a. Further, both narrow and wide grades displayed a similar amount of fine particles ($< 20 \mu\text{m}$) after crushing, Fig. 16 b. The similar crushing behavior can be attributed to the similar particle shape and residual crystal growth defects of both the wide and narrow grades. The wide particle size distribution allowed a higher packing density which dissipated the force onto a greater number of intra-particle contact points and reduced particle fracture.

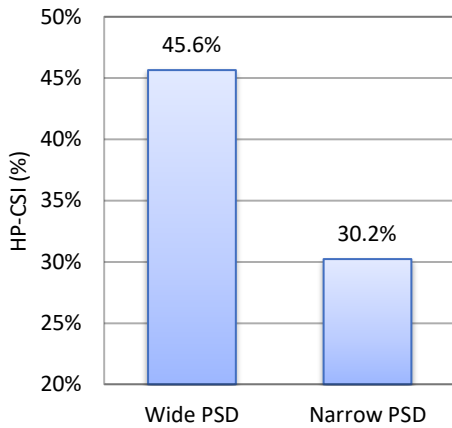


Fig. 16 a – HP-CSI with PSD width

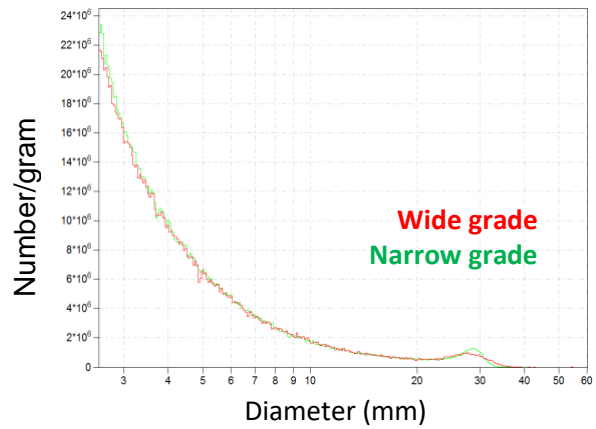
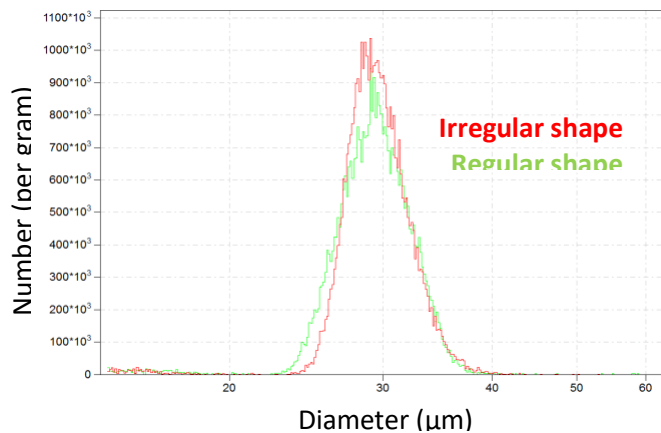


Fig. 16 b – PSD after crushing

b) Effect of particle shape on HP-SCI

Particle shape may be a factor in how particles arrange (pack) under pressure and how stresses are distributed within the particles. Two lots (batches) of metal bond diamond powder were graded to similar particle size, Fig. 17 and characterized by optical microscopy, Fig. 18. The average aspect ratio – AR (length/width), was determined to be 0.751 ± 0.096 and 0.657 ± 0.133 , for the regular and irregular shaped samples, respectively.



Sample	Diameter (µm)		
	5%	50%	95%
Regular shape	25.21	29.42	34.16
Irregular shape	26.02	29.27	34.04

Fig. 17 – Particle size distributions of 30 µm diamond samples – regular vs. irregular shape

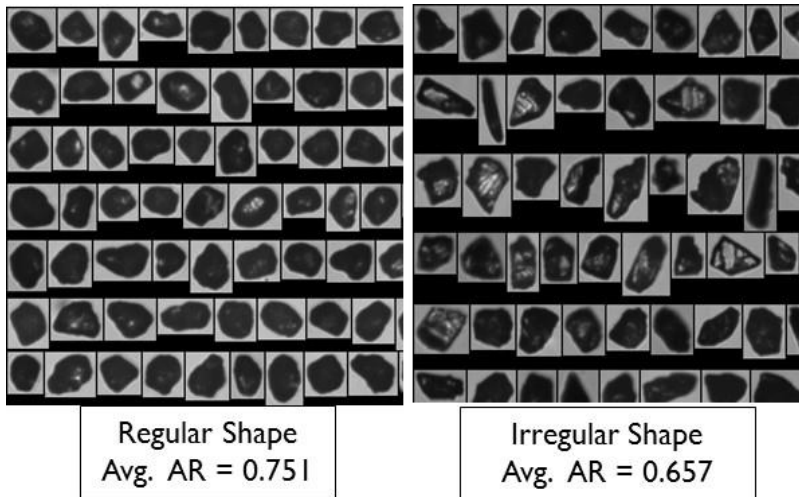


Fig. 18 – Particle shape analysis of 30 μm diamond samples – regular vs. irregular shape

After crushing, the irregular shape diamond powder sample displayed a significantly reduced HP-CSI than the regularly shaped diamond powder sample, Fig. 19, and generated more fine particles (< 10 μm), Fig. 20. The irregular shaped particles may have fractured more frequently due to the lower particle packing density as well as stress concentration on sharp points and edges. The fragmentation of shales and chipping of sharp corners and edges may have caused the increase in fine particle generation.

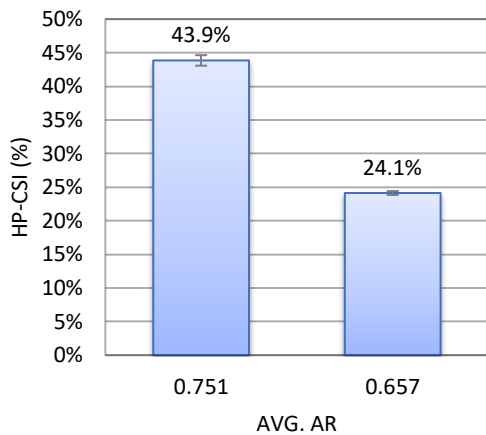


Fig. 19 – HP-CSI with particle shape (AR)

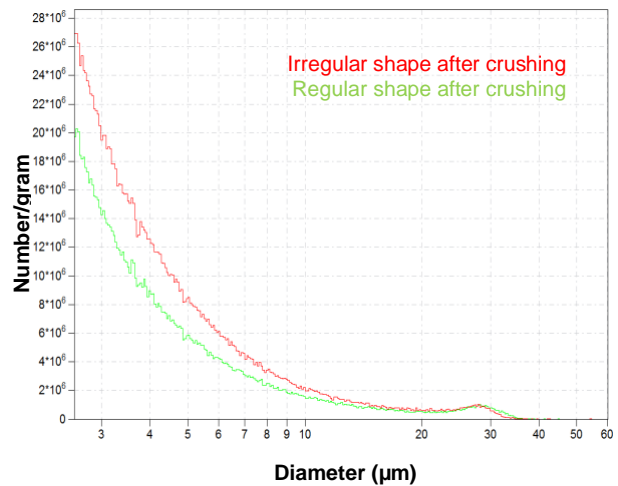


Fig. 20 – PSD after crushing

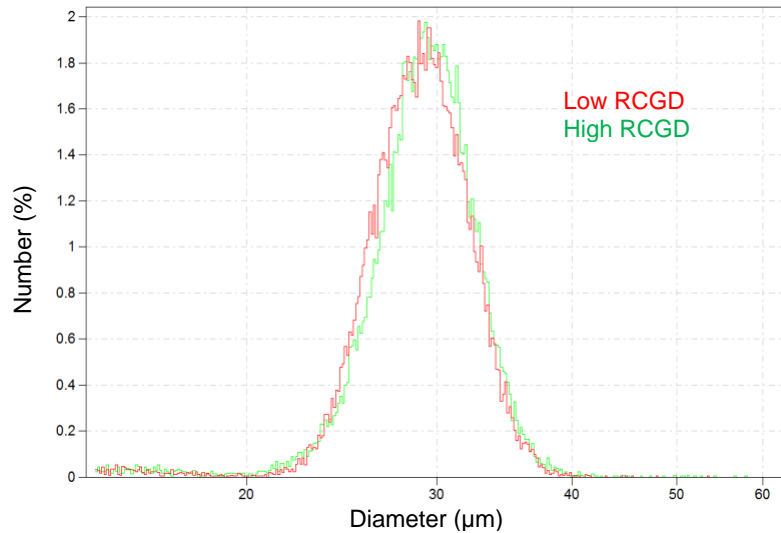
c) Effect of residual crystal growth defects on HP-CSI

Crystallographic defects, or crystal growth defects (CGD), of diamond are the result of the nucleation and crystal growth processes that govern the catalytic high pressure-high temperature (HPHT) graphite to diamond transformation (so called diamond synthesis process). Crystallographic defects (substitutional or interstitial impurities, vacancies, dislocations, etc.), are

sources of mechanical stresses, thus contributing to mechanical strength and fracture characteristics of monocrystalline diamond particles. Following the micronizing process (mechanical size reduction, chemical, and thermal process steps), some of the initial crystal growth defects of the starting mesh diamond powder feed are transmitted to the resultant micron size diamond powder as residual crystal growth defects (RCGD).

Characterization of RCGD level was determined by diffuse reflectance Fourier transform infrared spectroscopy (DR-FTIR). From our previous work [3], the DR-FTIR baseline transmittance (BT) can be related to the level of RCGD contained within each particle of a powder sample. Low levels of RCGD translates into higher DR-FTIR baseline transmittance due to less scatter and absorption of IR light by defects, while high levels of RCGD produce more scatter and absorption of IR light with a corresponding low DR-FTIR baseline transmittance.

To study how RCGD may affect fracture behavior at high pressure, two 30 μm diamond powder samples sharing almost identical PSD and particle shape were produced from two different powder feeds; one exhibiting high baseline transmittance (low level of RCGD), and the other exhibiting low baseline transmittance (high level of RCGD), Fig. 20 to Fig. 22.



Sample	Diameter on % (μm)		
	5%	50%	95%
Low RCGD	24.34	28.97	33.94
High RCGD	24.04	29.33	34.33

Fig. 20 – Particle size distributions of 30 μm diamond samples – high and low RCGD

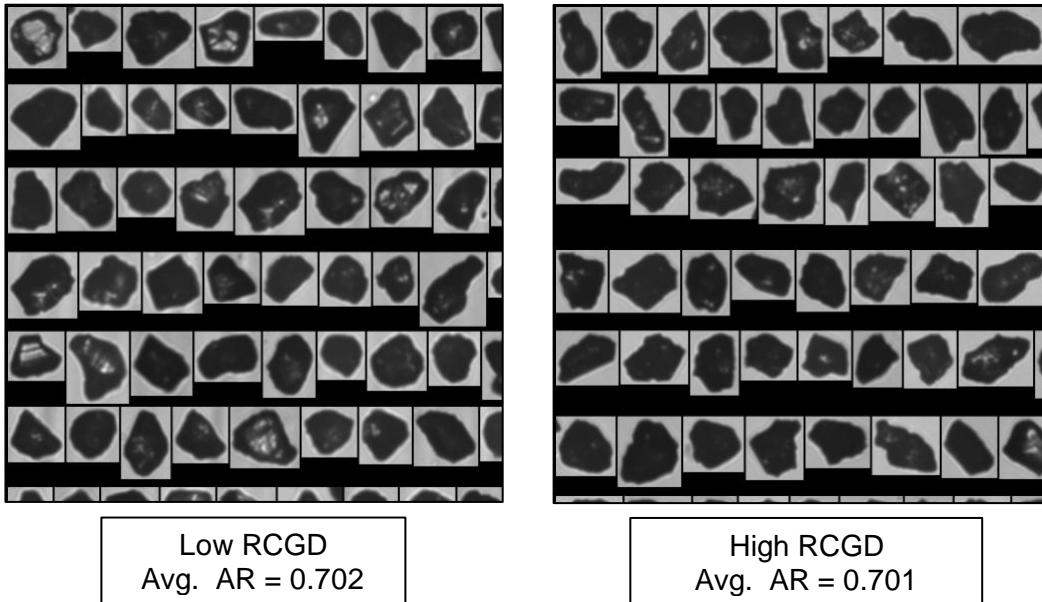


Fig. 21 – Shape characterization of 30 μm diamond samples – high and low RCGD

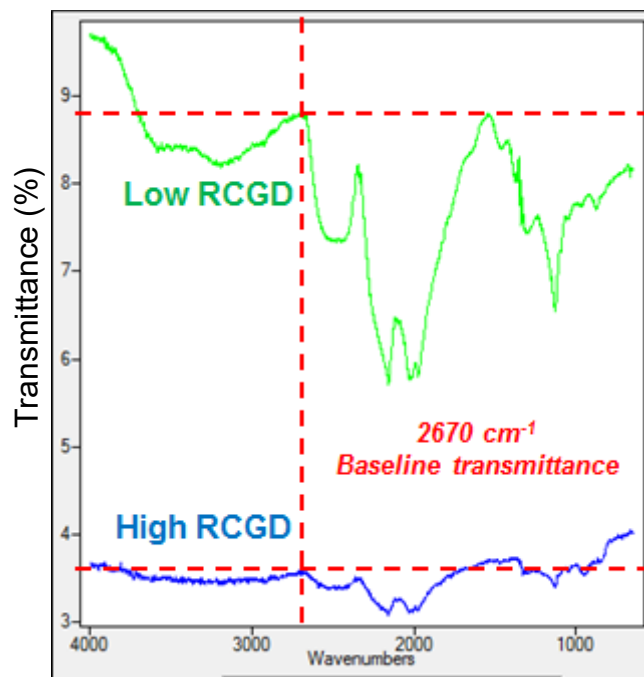


Fig. 22 – DR-FTIR characterization of 30 μm diamond samples – high and low RCGD

After crushing under HP, the high RCGD sample had a lower HP-CSI than the similarly sized and shaped low RCGD sample, Fig. 23. As expected, the more defective particles had a higher probability of fracture under similar pressure than a less defective particles. Further, the mode of fracture was similar, i.e. both samples generated similar amounts of fine particles, Fig. 24.

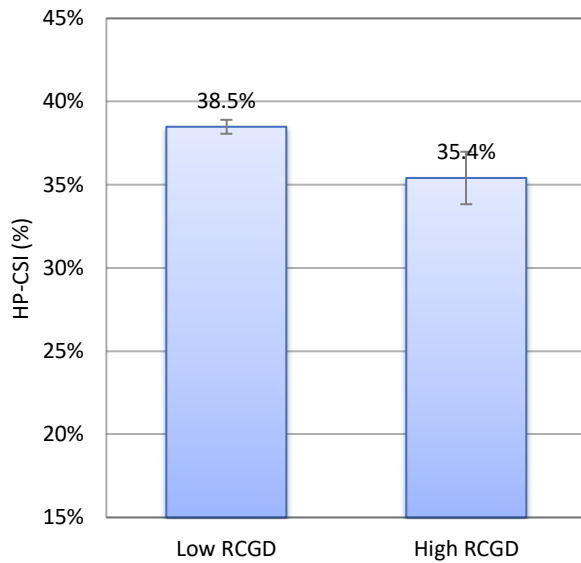


Fig. 23 – HP-CSI with level of RCGD

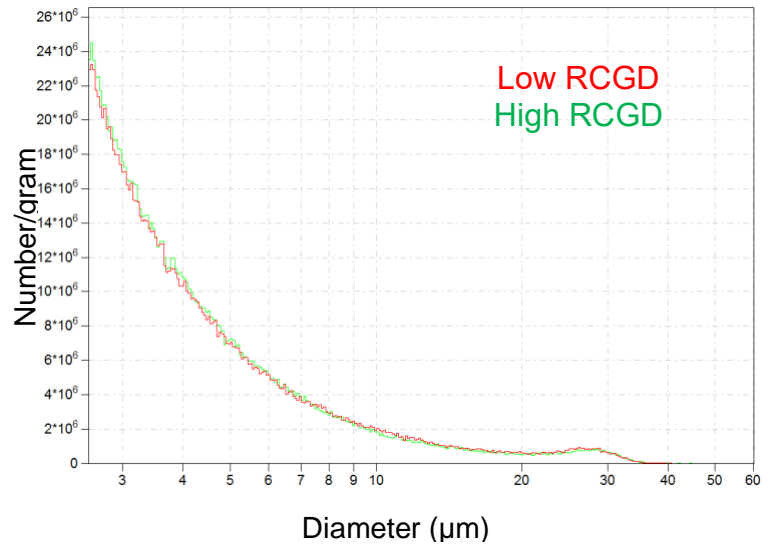


Fig. 24 – PSD after crushing

4 Conclusions

In this paper, we present a novel technique and the associated apparatus developed to assess the crushing strength (expressed as high pressure crushing strength index, HP-CSI) and mode (expressed as the amount and size distribution of fine particles generated), following high pressure treatment of the precursor micron diamond powder used for HPHT sintering of polycrystalline diamond compacts (i.e. PDC cutters for oil and gas drilling, PDC tool blanks and dies, etc.).

An opposed anvils high pressure apparatus, which incorporates a pair of PDC-WC composite anvils, was developed to simulate the high pressure environment, experienced by micron diamond powder during pressure ramp-up in HPHT sintering process of PDC.

The HP-CSI results obtained using the HP apparatus developed, are consistent with HP-CSI results acquired on the same diamond samples, using an industrial cubic press for PDC sintering. The high pressure crushing strength technique is flexible in the range of applied load (pressure), dwell time and size of micron diamond powder that may be studied.

Using the technique developed to assess the crushing strength of micron diamond powder under static high pressure, it was found that, as expected, characteristics of micron diamond powder affect their failure behavior at high pressure and ambient temperature. Wider particle size distribution induces increased packing density, and reduced fracture of diamond particles. Irregular particle shapes (low AR) determine increased fracture of diamond particles, with tendency to generate larger amount of fine particles.

The concentration of residual crystal growth defects (RCGD), affect the fracture strength of diamond particles. High concentration of RCGD, results in low fracture strength of diamond particles.

Using the HP-CSI technique, precursor micron diamond powders for HPHT sintering of PDC, may be further developed to ensure predictable and consistent performance under the high pressure conditions, particular to different PDC sintering processes.

5 References

[1] Benea, I., Griffin, S., *“Mechanical strength and fracture characteristics of micron diamond”*, Industrial Diamond Review, (2003) pp. 53-60

[2] Benea, I et al. *US Patent 7,275,446, Oct. 2, 2007*

[3] Benea, I., Rosczyk, B., *“Crystallographic defects and mechanical strength of micron size monocrystalline diamond”*, International Technical Conference on Diamond, Cubic Boron Nitride and Their Applications (INTERTECH 2013), 6-8 May 2013, Baltimore, Maryland, USA. ISBN: 9781510803619

Acknowledgments:

The authors acknowledge I. Popescu, PhD. – Polytechnic Institute, Bucharest, Romania, for his help with high pressure apparatus design.